

Chromatographic Separation and Multicollection-ICPMS Analysis of Iron. Investigating Mass-Dependent and -Independent Isotope Effects

Nicolas Dauphas,^{*,†,‡,§,||} Philip E. Janney,^{§,||} Ruslan A. Mendybaev,^{†,||} Meenakshi Wadhwa,^{§,||} Frank M. Richter,^{†,||} Andrew M. Davis,^{†,‡,||} Mark van Zuilen,[⊥] Rebekah Hines,^{§,||} and C. Nicole Foley^{§,||}

Department of the Geophysical Sciences, The University of Chicago, 5734 South Ellis Avenue, Chicago, Illinois 60637, Enrico Fermi Institute, The University of Chicago, 5640 South Ellis Avenue, Chicago, Illinois 60637, Department of Geology, The Field Museum, 1400 South Lake Shore Drive, Chicago, Illinois 60605, Chicago Center for Cosmochemistry, 5640 South Ellis Avenue, Chicago, Illinois 60637, and Centre de Recherches Pétrographiques et Géochimiques, 15 rue Notre Dame des Pauvres, BP 20, 54501 Vandoeuvre-lès-Nancy Cedex, France

A procedure was developed that allows precise determination of Fe isotopic composition. Purification of Fe was achieved by ion chromatography on AG1-X8 strongly basic anion-exchange resin. No isotopic fractionation is associated with column chemistry within 0.02‰/amu at 2σ . The isotopic composition was measured with a Micromass IsoProbe multicollection inductively coupled plasma hexapole mass spectrometer. The Fe isotopic composition of the Orgueil CI1 carbonaceous chondrite, which best approximates the solar composition, is indistinguishable from that of IRMM-014 ($-0.005 \pm 0.017\text{‰}/\text{amu}$). The IRMM-014 reference material is therefore used for normalization of the isotopic ratios. The protocol for analyzing mass-dependent variations is validated by measuring geostandards (IF-G, DTS-2, BCR-2, AGV-2) and heavily fractionated Fe left after vacuum evaporation of molten wüstite (FeO) and solar (MgO-Al₂O₃-SiO₂-CaO-FeO in chondritic proportions) compositions. It is shown that the isotopic composition of Fe during evaporation of FeO follows a Rayleigh distillation with a fractionation factor α equal to $(m_1/m_2)^{1/2}$, where m_1 and m_2 are the masses of the considered isotopes. This agrees with earlier measurements and theoretical expectations. The isotopic composition of Fe left after vacuum evaporation of solar composition also follows a Rayleigh distillation but with a fractionation factor ($1.013\,22 \pm 0.000\,67$ for the $^{56}\text{Fe}/^{54}\text{Fe}$ ratio) that is lower than the square root of the masses ($1.018\,35$). The protocol for analyzing mass-independent variations is validated by measuring terrestrial rocks that are not expected to show departure from mass-dependent fractionation. After internal normalization of the $^{57}\text{Fe}/^{54}\text{Fe}$ ratio, the isotopic composition

of Fe can be measured accurately with precisions of 0.2‰ and 0.5‰ at 2σ for $^{56}\text{Fe}/^{54}\text{Fe}$ and $^{58}\text{Fe}/^{54}\text{Fe}$ ratios, respectively (‰ refers to relative variations in parts per 10 000). For ^{58}Fe , this precision is an order of magnitude better than what had been achieved before. The method is applied to rocks that could potentially exhibit mass-independent effects, meteorites and Archaean terrestrial samples. The isotopic composition of a 3.8-Ga-old banded iron formation from Isua (IF-G, Greenland), and quartz–pyroxene rocks from Akilia and Innersuartuut (GR91-26 and SM/GR/171770, Greenland) are normal within uncertainties. Similarly, the Orgueil (CI1), Allende (CV3.2), Eagle Station (ESPAL), Brenham (MGPAL), and Old Woman (IIAB) meteorites do not show any mass-independent effect.

Iron ($Z = 26$) possesses four stable isotopes, 54, 56, 57, and 58, with natural abundances of 5.845, 91.754, 2.1191, and 0.2819%, respectively.¹ After hydrogen, helium, oxygen, carbon, neon, nitrogen, magnesium, and silicon, it is the ninth most abundant element by atom in the universe.² This element was predominantly synthesized in Si burning during supernova explosions in the form of radioactive ^{56}Ni that subsequently decayed to ^{56}Fe .³ Natural isotope variations of Fe can be divided into two categories, mass-dependent and mass-independent effects. The first category groups all phenomena for which the variation of isotope abundances is governed by mass difference. The second category groups all processes that do not obey this rule. Both types of Fe isotopic variations have already been documented in nature.

With a 50% condensation temperature of 1473 K under canonical conditions for the nebula, Fe is classified as a moderately volatile element.⁴ During evaporation of liquid droplets in a gas of low Fe partial pressure, Fe is lost and can be isotopically

* To whom correspondence should be addressed. E-mail: dauphas@uchicago.edu.

[†] Department of the Geophysical Sciences, The University of Chicago.

[‡] Enrico Fermi Institute, The University of Chicago.

[§] The Field Museum.

^{||} Chicago Center for Cosmochemistry.

[⊥] Centre de Recherches Pétrographiques et Géochimiques.

(1) Taylor, P. D. P.; Maeck, R.; De Bièvre, P. *Int. J. Mass Spectrom. Ion Processes* **1992**, *121*, 111–125.

(2) Anders, E.; Grevesse, N. *Geochim. Cosmochim. Acta* **1989**, *53*, 197–214.

(3) Clayton, D. D. *Meteorit. Planet. Sci.* **1999**, *34*, A145–A160.

(4) Grossman, L. *Geochim. Cosmochim. Acta* **36**, 597–619.

fractionated in a mass-dependent manner.⁵ Chondrules,^{6–9} cosmic spherules,^{10–12} lunar soils,¹³ and possibly planets¹⁴ show such effects. Iron is also known to be mass fractionated in geological environments at low and high temperatures.^{15,16} Although the origins of the variations observed in terrestrial surface rocks and fluids are debated, various abiotic processes operating at low temperature can induce isotopic fractionation.^{15–23} High-temperature partitioning between mantle minerals is known to fractionate the isotopic composition of Fe.^{15,24,25} Iron is also affected by biological processes when assimilated, when used in energy generation, or when involved in photosynthesis.^{15,16,26–29}

Departure from mass fractionation has not yet been found in terrestrial samples and has so far been documented only in components within a few extraterrestrial samples. Although the theoretical basis for understanding these effects is uncertain, some chemical reactions can induce mass-independent variations in the isotopes of some elements.^{30,31} Such exotic effects have never been documented for Fe. Nuclear processes can also alter the isotopic compositions of elements. The isotopes of Fe were not synthesized at the same time and place in the galaxy. If all the stellar sources that contributed to the nucleosynthesis of Fe were not homogenized in the protosolar nebula, then departure from mass

fractionation would arise. This is what is observed in some refractory mineral assemblages (Ca–Al-rich inclusions) in meteorites.³² These anomalies affect predominantly ⁵⁸Fe, which is also the rarest of all Fe isotopes.

Iron isotopic determinations have long been hampered by its low ionization efficiency (first ionization potential 7.870 eV) and the difficulty in correcting instrumental mass fractionation (*f*). The recent advent of multicollection inductively coupled plasma mass spectrometers (MC-ICPMS) has extended dramatically the range of applications of mass fractionation of Fe as a tracer in natural systems. The main difficulties with this new generation of instruments lie in the presence of large isobaric interferences on some of the Fe isotopes originating from neighbor elements that are efficiently ionized (⁵⁴Cr⁺ on 54 and ⁵⁸Ni⁺ on 58), hydrides of the analyte (⁵⁶Fe¹H⁺ on 57 and ⁵⁷Fe¹H⁺ on 58), and most importantly molecular interferences from the Ar plasma (⁴⁰Ar¹⁴N⁺ on 54, ⁴⁰Ar¹⁶O⁺ on 56, and ⁴⁰Ar¹⁶O¹H⁺ on 57). The interferences from Cr and Ni can be reduced to insignificant levels by chemical separation. In addition, multicollection allows one to monitor and correct for the possible presence of ⁵⁴Cr and ⁵⁸Ni with other Cr and Ni isotopes. Hydride interferences are not a major problem because the FeH/Fe ratio is typically small and remains constant. Various strategies have been adopted to reduce molecular interferences originating from the Ar plasma. These involve sample desolvation,^{17,21,33} collision cells,^{16,22,34,35} cold plasma,^{8,28} and high resolution.^{36,37}

In the present contribution, two ion-exchange procedures for chemical separation of Fe are presented. Both use concentrated HCl as a fixation medium. One uses cation exchange (AG50W-X4 100–200 mesh) while the other relies on anion exchange (AG1-X8 200–400 mesh). Two protocols aimed at measuring mass fractionation and anomalous effects for Fe are then discussed. Note that all uncertainties are given as 95% confidence intervals.

EXPERIMENTAL SECTION

Separation Chemistry. Sample handling and chemistry were performed in a class 1000 clean laboratory at the Field Museum. Hydrochloric acid was purified by quadruple sub-boiling distillation in Teflon. Teflon beakers were used exclusively. After bulk digestion, the sample was dissolved in aqua regia and evaporated to dryness. The sample was then dissolved in HNO₃–HCl–HClO₄ and was again evaporated to dryness. This was done to ensure that Fe was present as ferric iron in the solution before loading on the resin.

Anion Exchange. The most widely used chemical procedure for separating Fe from potential isobaric interferences is based on anion exchange in an HCl medium. The sorption of Fe(III) on anion exchangers increases steeply with the HCl molarity, from $K_D < 1$ at low concentration to $K_D > 10^4$ at high concentration

- (5) Wang, J.; Davis, A. M.; Clayton, R. N.; Mayeda, T. K. *Lunar Planet. Sci.* **1994**, XXV, 1459–1460.
- (6) Zhu, X. K.; Guo, Y.; O'Nions, R. K.; Young, E. D.; Ash, R. D. *Nature* **2001**, 412, 311–313.
- (7) Mullane, E.; Russell, S. S.; Weiss, D.; Gounelle, M.; Mason, T. F. D.; Jeffries, T. E. *Meteorit. Planet. Sci.* **2001**, 36, A142–A143.
- (8) Kehm, K.; Hauri, E. H.; Alexander, C. M. O'D.; Carlson, R. W. *Geochim. Cosmochim. Acta* **2003**, 67, 2879–2891.
- (9) Alexander, C. M. O'D.; Wang, J. *Meteorit. Planet. Sci.* **2001**, 36, 419–428.
- (10) Davis, A. M.; Clayton, R. N.; Mayeda, T. K.; Brownlee, D. E. *Lunar Planet. Sci.* **1991**, XXII, 281–282.
- (11) Herzog, G. F.; Xue, S.; Hall, G. S.; Nyquist, L. E.; Shih, C.-Y.; Wiesmann, H.; Brownlee, D. E. *Geochim. Cosmochim. Acta* **1999**, 63, 1443–1457.
- (12) Alexander, C. M. O'D.; Taylor, S.; Delaney, J. S.; Ma, P.; Herzog, G. F. *Geochim. Cosmochim. Acta* **2002**, 66, 173–183.
- (13) Wiesli, R. A.; Beard, B. L.; Taylor, L. A.; Johnson, C. M. *Earth Planet. Sci. Lett.* **2003**, 216, 457–465.
- (14) Poitrasson, F.; Halliday, A. N.; Lee, D.-C.; Levasseur, S.; Teutsch, N. *Earth Planet. Sci. Lett.*, **2004**, 223, 253–266.
- (15) Zhu, X. K.; Guo, Y.; Williams, R. J. P.; O'Nions, R. K.; Matthews, A.; Belshaw, N. S.; Canters, G. W.; de Waal, E. C.; Weser, U.; Burgess, B. K.; Salvato, B. *Earth Planet. Sci. Lett.* **2002**, 200, 47–62.
- (16) Beard, B. L.; Johnson, C. M.; Skulan, J. L.; Nealson, K. H.; Cox, L.; Sun, H. *Chem. Geol.* **2003**, 195, 87–117.
- (17) Roe, J. E.; Anbar, A. D.; Barling, J. *Chem. Geol.* **2003**, 195, 69–85.
- (18) Matthews, A.; Zhu, X.-K.; O'Nions, K. *Earth Planet. Sci. Lett.* **2001**, 192, 81–92.
- (19) Welch, S. A.; Beard, B. L.; Johnson, C. M.; Braterman, P. S. *Geochim. Cosmochim. Acta* **2003**, 67, 4231–4250.
- (20) Bullen, T. D.; White, A. F.; Childs, C. W.; Vivit, D. V.; Schulz, M. S. *Geology* **2001**, 29, 699–702.
- (21) Sharma, M.; Polizzotto, M.; Anbar, A. D. *Earth Planet. Sci. Lett.* **2001**, 194, 39–51.
- (22) Rouxel, O.; Dobbek, N.; Ludden, J.; Fouquet, Y. *Chem. Geol.* **2003**, 202, 155–182.
- (23) Rouxel, O.; Fouquet, Y.; Ludden, J. *Geochim. Cosmochim. Acta* **2004**, 68, 2295–2311.
- (24) Williams, H. M.; McCammon, C. A.; Peslier, A. H.; Halliday, A. N.; Teutsch, N.; Levasseur, S.; Burg, J.-P. *Science* **2004**, 304, 1656–1659.
- (25) Beard, B. L.; Johnson, C. M. *Geochim. Cosmochim. Acta* **2003**, 67, A35.
- (26) Beard, B. L.; Johnson, C. M.; Cox, L.; Sun, H.; Nealson, K. H.; Aguilar, C. *Science* **1999**, 285, 1889–1892.
- (27) Brantley, S. L.; Liermann, L.; Bullen, T. D. *Geology* **2001**, 29, 535–538.
- (28) Walczyk, T.; von Blanckenburg, F. *Science* **2002**, 295, 2065–2066.
- (29) Croal, L. R.; Johnson, C. M.; Beard, B. L.; Newman, D. K. *Geochim. Cosmochim. Acta* **2004**, 68, 1227–1242.
- (30) Thieme, M. H. *Science* **1999**, 283, 341–345.
- (31) Farquhar, J.; Wing, B. A. *Earth Planet. Sci. Lett.* **2003**, 213, 1–13.

- (32) Völkner, J.; Papanastassiou, D. A. *Astrophys. J.* **1989**, 347, L43–L46.
- (33) Belshaw, N. S.; Zhu, X. K.; Guo, Y.; O'Nions, R. K. *Int. J. Mass Spectrom. Ion Processes* **1999**, 197, 191–195.
- (34) Dauphas, N.; Rouxel, O.; Davis, A. M.; Lewis, R. S.; Wadhwa, M.; Marty, B.; Reisberg, L.; Janney, P. E.; Zimmermann, C. *Lunar Planet. Sci.* **2003**, XXXIV, 1807.
- (35) Mullane, E.; Russell, S. S.; Gounelle, M.; Mason, T.; Din, V.; Weiss, D.; Coles, B. In *Plasma Source Mass Spectrometry: Applications and Emerging Technologies*; The Royal Society of Chemistry: London, 2003; pp 351–361.
- (36) Weyer, S.; Schwieters, J. B. *Int. J. Mass Spectrom.* **2003**, 226, 355–368.
- (37) Arnold, G. L.; Weyer, S.; Anbar, A. D. *Anal. Chem.* **2004**, 76, 322–327.

Table 1. Yields and Isotopic Fractionation for Anion (A) and Cation (C) Exchange Separation^a

	A 1	A 2	A 3	C 1	C 2	C 3
<i>Y</i>	>0.98	>0.98	>0.98	0.919 ± 0.020	0.920 ± 0.020	0.932 ± 0.020
<i>L</i>	0.0019	0.0014	0.0017	0.0115	0.0058	0.0050
<i>F</i>	-0.009	-0.024	0.014	-0.009	-0.009	0.008
\pm	0.020	0.036	0.159	0.075	0.050	0.059
\bar{F}		-0.012 ± 0.018			-0.003 ± 0.034	

^a The yield *Y* is the fraction of Fe recovered in the iron cut, *L* is the fraction of Fe lost in the matrix cut, *F* is the column isotopic fractionation in ‰/amu, and \bar{F} is the weighted ($1/\sigma^2$) average column fractionation. Uncertainties are 2σ . The fraction of Fe remaining on the column after the elution is completed is $1 - Y - L$.

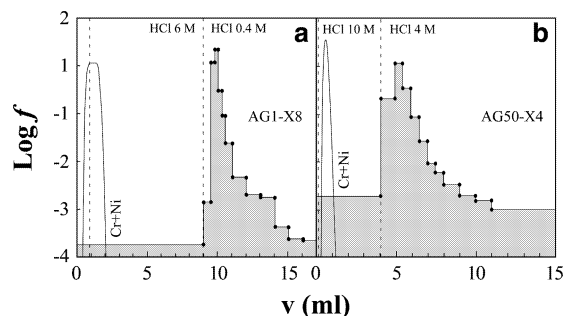


Figure 1. Elution sequences of Fe on AG1-X8 200–400-mesh anion (a) and AG50W-X4 100–200-mesh cation (b) exchange resins. The volume of the anion-exchange column is 1 mL ($2.0 \text{ cm} \times \text{i.d. } 0.8 \text{ cm}$). The volume of the cation-exchange resin is 1.6 mL when hydrated ($3.2 \text{ cm} \times \text{i.d. } 0.8 \text{ cm}$). Elution curves for Cr and Ni, which form isobaric interferences with Fe isotopes, were simulated using the theoretical plate model of chromatography and available partition coefficients.

(K_D is the resin/liquid partition coefficient).³⁸ In these conditions, Ni and Cr (the direct isobars of Fe) are not quantitatively retained. Following Strelow,³⁹ Fe was fixed on anion-exchange resin in concentrated HCl and was then eluted at low HCl molarity.

Disposable Bio-Rad Poly-Prep columns were filled with 1 mL ($2.0 \text{ cm} \times \text{i.d. } 0.8 \text{ cm}$) of AG1-X8 200–400 mesh chloride form resin. These were then cleaned and conditioned by running 10 mL of H_2O , 5 mL of 1 M HNO_3 , 10 mL of H_2O , 10 mL of 0.4 M HCl, 5 mL of H_2O , and 2 mL of 6 M HCl through them. Sample solutions were loaded in 0.1–1.0 mL of 6 M HCl. At this molarity, the partition coefficient of Fe is higher than 10^3 in favor of the resin. Matrix elements and isobars of Fe were eluted in 8 mL of 6 M HCl, in a sequence 0.5, 0.5, 1, 2, and 4 mL. For samples containing large amounts of copper, this can be extended to 15 mL. When investigating mass-independent effects, it can even be increased to 25 mL. Iron was eluted in 9 mL of 0.4 M HCl, in a sequence 0.5, 0.5, 1, 1, 2, and 4 mL. As illustrated in Figure 1a, the behavior of Fe agrees with expectations. The procedural blank is 20 ng, which is comparable to a typical rock dissolution blank of 30 ng. The yield is higher than 98% (Table 1). Less than 0.2% of the total Fe is lost during matrix elution.

Anion-exchange resins are known to fractionate Fe isotopes.¹⁷ Although the equilibrium fractionation factor is small, isotopic effects are amplified by the chromatographic process. It is therefore necessary to test whether Fe eluted from the column is fractionated relative to its initial isotopic composition. This is not only important for analyzing the mass-dependent component of

the variations. To detect anomalous effects, it is required to correct for natural (N), laboratory (L), and instrumental (I) mass fractionation. The parametrized law⁴⁰ governing isotopic mass fractionation on the instrument (f_i) is applied for correcting the total mass fractionation $N + L + I$. If $N + L$ is large and the variations are not adequately described by f_i , then spurious mass-independent effects may arise. The isotopic fractionation introduced by column chromatography (*L*) should therefore be minimized. The average isotopic fractionation measured on three distinct anion-exchange columns (A in Table 1) is $-0.012 \pm 0.018\text{‰/amu}$, indistinguishable from zero within uncertainties. This shows that there is no isotopic fractionation of Fe within 0.02‰/amu during chemical separation on the anion-exchange columns.

Cation Exchange. The simplicity of the separation of Fe on anion-exchange resin is attested to by its widespread use. However, as with any chemistry, it cannot easily handle every possible sample. In addition, for some specific applications requiring especially high purity of Fe, crossing the selectivities of the two types of resins can prove fruitful. A scheme based on AG50W-X4 100–200-mesh hydrogen form resin was investigated for purifying Fe. The partition coefficient of ferric iron on cation-exchange resins^{38,41} is high at low HCl molarity (close to 10^2); it assumes a minimum value for moderate HCl concentration (<1 at 4 M) and increases again to very high values at high HCl concentration ($>10^2$ for molarities higher than 8 M). In contrast, Cr and Ni have partition coefficients that steadily decrease with increasing HCl concentration (<1 for molarities higher than 4 M). Ferric iron was therefore fixed on cation-exchange resin at high HCl molarity and was subsequently eluted at 4 M HCl.

Disposable Bio-Rad Poly-Prep columns were filled with 1.6 mL ($3.2 \text{ cm} \times \text{i.d. } 0.8 \text{ cm}$) of hydrated AG50W-X4 100–200-mesh hydrogen form resin. These were then cleaned and conditioned by running 10 mL of H_2O , 5 mL of 4 M HCl, 10 mL of H_2O , 10 mL of 4 M HCl, 5 mL of H_2O , and 2 mL of 10 M HCl through them. After conditioning in concentrated HCl, the resin dehydrates and the volume reduces to 1 mL. Approximately 30 min after conditioning, the sample is loaded dropwise in $100 \mu\text{L}$ of 10 M HCl. Due to the strong dehydration of the resin in concentrated HCl, exchange kinetics are dramatically slowed.⁴¹ After loading, the resin was allowed to sit for 2 h to allow diffusion of Fe in resin pores. If the matrix elution is performed immediately after loading, Fe is not quantitatively retained. Matrix elements and isobars of Fe were then eluted in 4 mL of 10 M HCl at a controlled

(38) Helfferich, F. G. *Ion Exchange*; McGraw-Hill: New York, 1962.

(39) Strelow, F. W. E. *Talanta* **1980**, *27*, 727–732.

(40) Maréchal, C. N.; Télouk, P.; Albarède, F. *Chem. Geol.* **1999**, *156*, 251–273.

(41) Nelson, F.; Murase, T.; Kraus, K. A. *J. Chromatogr.* **1964**, *13*, 503–535.

introduction rate of 100 $\mu\text{L}/\text{min}$ (achieved by overlying the cation-exchange column with an anion-exchange column containing 3 mL of clean resin). Iron was then eluted with 11 mL of 4 M HCl in a sequence 1 mL, wait 30 min, 1, 2, 3, and 4 mL. As illustrated in Figure 1b, the elution curve of Fe is not symmetric and tailing is present. When loading 1000 μg of Fe, the yield is 92–93%. Part of the Fe was lost during matrix elution, and part was not eluted in 4 M HCl. The yield was found to decrease with increasing amounts of Fe loaded (practically, the load should not exceed 1000 μg of Fe). This effect must be due to saturation of the outer shells of the resin spheres (the inner sites are unavailable to exchange due to slow diffusion). Although the recovery is not total, the measured column fractionation is $-0.003 \pm 0.034\text{‰}/\text{amu}$ at 2σ , indistinguishable from 0. Another procedure was tested for eluting Fe out of the cation-exchange resin with nitric acid (2 mL of H_2O , 11 mL of HNO_3). The average yield and mass fractionation based on three column replicates are $96.6 \pm 1.2\%$ and $0.009 \pm 0.036\text{‰}/\text{amu}$, respectively. Again, the yield is not 100%, but no fractionation is associated with Fe loss.

The procedure based on anion exchange is much simpler than that based on cation exchange. For this reason, only the first one will be used in the present article.

Mass Spectrometry. A variety of analytical techniques have been used for determining the isotopic composition of Fe, including P-TIMS^{11,20,26,27,32,42} and SIMS.^{5,9,10,12} These two methods are limited by the low ionization efficiency of Fe and the difficulty in accurately and precisely correcting for instrumental mass fractionation. The recent advent of MC-ICPMS has dramatically extended the range of applications of Fe isotopes.^{6–8,13–19,21–25,28,29,33–37} The Fe isotope determinations reported here were performed at the Isotope Geochemistry Laboratory of the Field Museum (Chicago), on a Micromass IsoProbe MC-ICPMS. This instrument is equipped with nine Faraday collectors (an axial collector A, two collectors on the low-mass side L3 and L2, and 6 collectors on the high-mass side H1–H6), allowing the simultaneous determination of all Fe isotopes and monitoring of potential isobars of Fe. The singly charged cations of ^{53}Cr , $^{54}\text{Cr} + ^{54}\text{Fe}$, ^{56}Fe , ^{57}Fe , $^{58}\text{Fe} + ^{58}\text{Ni}$, and ^{60}Ni were measured on the L3, L2, A, H1, H2, and H6 collectors, respectively. Despite the fact that the sampler, skimmer, and collimator cones are made of nickel, the Ni peak at mass 58 in blank solutions was negligibly small. Chromium and nickel isobaric interferences on Fe isotopes were monitored and corrected. Instrumental mass fractionation was first calculated based on the measured $^{56}\text{Fe}/^{57}\text{Fe}$ ratio and a terrestrial reference composition¹ taken to be representative of the unfractionated composition of the sample. Note that the difference between measured and true isotopic compositions tends to be much larger than the natural Fe isotopic variations between samples. The calculated instrumental mass bias was used to estimate instrumentally fractionated $^{54}\text{Cr}/^{53}\text{Cr}$ and $^{58}\text{Ni}/^{60}\text{Ni}$ ratios,^{43,44} using the exponential law.⁴⁰ These fractionated ratios were subsequently multiplied by the intensities measured at masses 53 and 60 to calculate and subtract the contributions of Cr and Ni on Fe isotopes. For Mo, such a correction has been shown to be accurate up to extremely high interference levels.⁴⁵

Determination of Fe isotope abundances is complicated by the presence of molecular ions containing Ar, including ArN^+ on 54, ArO^+ on 56, and ArOH^+ on 57. Various strategies have been adopted in the past to reduce these interferences, including sample desolvation,^{17,21,33} collision cells,^{16,22,34,35} cold plasma,^{8,28} and high resolution.^{36,37} In the present study, Fe was run at comparatively high concentration, using a desolvating nebulizer, and Ar and H_2 were introduced in the hexapole collision cell of the mass spectrometer. The instrument was run in two different modes, depending on whether mass-dependent or -independent variations were being investigated.

Mass-Dependent Effects and Reference Materials. When investigating mass fractionation on ICPMS, it is important to ensure that no isobaric interferences are present, that the sample solution is devoid of matrix elements that could modify the instrumental mass fractionation I , and that I remains stable while analyzing standard solutions. The sample solution (1 ppm Fe in 0.5 M HNO_3) was introduced through a Teflon nebulizer (100 $\mu\text{L}/\text{min}$) in a Cetac Aridus desolvating system. Only Ar (3 l/min) was introduced in the desolvating system (N_2 was avoided due to the possible formation of ArN^+ in the plasma torch). The mass spectrometer was run in soft extraction (a mode in which a small positive voltage is applied to the cones that reduces the transmission of molecular ions), with the plasma shield on, at an operating torch power of 1500 W. The hexapole rf amplitude was set at 40%, which promotes transmission of intermediate mass ions and further reduces the signal-to-noise ratio in the Fe mass region, specifically at mass 57. Following earlier work,⁴⁶ Ar (1 mL/min) and H_2 (1–1.8 mL/min) were introduced in the hexapole collision cell in order to (i) reduce the energy spread of the incident ions through partial thermalization with the ambient gas and (ii) reduce argide interferences on Fe isotopes to insignificant levels, except for $^{40}\text{Ar}^{16}\text{O}^+\text{H}^+$. The persistent ArOH^+ interference at mass 57 is not formed in the hexapole collision cell but rather in the plasma torch.¹⁶ After optimization of the nebulizer gas, the torch position, and ion optics, the values of the mass resolution slit and slit lens were modified to get ~ 4 V/ppm on the axial collector at mass 56 with a $10^{11} \Omega$ resistor. This increases the signal-to-noise ratio compared to an instrument run at full transmission with an equivalent measured ion current. The calculated yield is 1.4×10^{-5} Fe^+ ion counted/Fe atom consumed. The extraction voltage is not lowered in soft extraction mode because of rapid buildup of deposits on the cones and, consequently, loss of signal sensitivity and worsening of isotope ratio precision. The extraction voltage was set at -6000 V.

A modified Cetac autosampler that can accommodate 10-mL Teflon beakers was used throughout this study. The analysis was done by bracketing sample analysis with standard measurements. Between each analysis, the system was rinsed in 0.5 M HNO_3 for 240 s. A blank solution (0.5 M HNO_3 intensity I_B at a given mass) was introduced and integrated for one minute (the ^{56}Fe peak was centered manually by adjusting the high tension). The analyte solution (intensity I_A at a given mass) was then introduced (admittance delay 90 s). The peak position was automatically

(42) Johnson, C. M.; Beard, B. L. *Int. J. Mass Spectrom.* **1999**, *193*, 87–99.

(43) Shields, W. R.; Murphy, T. J.; Catanzaro, E. J.; Garner, E. L. *J. Res. Natl. Bur. Stand.* **1966**, *70A*, 193–197.

(44) Gramlich, J. W.; Machlan, L. A.; Barnes, I. L.; Paulsen, P. J. *J. Res. Natl. Bur. Stand.* **1989**, *94*, 347–356.

(45) Dauphas, N.; Reisberg, L.; Marty, B. *Anal. Chem.* **2001**, *73*, 2613–2616.

(46) Meffan-Main, S.; Palacz, Z.; Turner, P. *Geoscience 2000*, Manchester, U.K., April 2000.

Table 2. Sample–Standard Bracketing Schemes^a

	std	sample	std
intensity	I_1	I	I_2
time	t_1	t	t_2
isotope ratio	R_1	R	R_2
R_{STD} (I -interpolated)	$R_1 + [(R_2 - R_1)/(I_2 - I_1)](I - I_1)$		
R_{STD} (t -interpolated)	$R_1 + [(R_2 - R_1)/(t_2 - t_1)](t - t_1)$		

^a The intensity interpolation assumes that there is a linear relationship between the isotopic composition and the measured intensity of ⁵⁶Fe. The time interpolation assumes that there is a linear relationship between the isotopic composition and the time of the measurement. The isotopic composition is expressed in δ notation, $\delta = (R/R_{STD} - 1) \times 10^3$, where R_{STD} is the interpolated standard composition.

centered by adjusting the magnetic field. The measurements were done in a sequence of 10–15 cycles, each cycle integrating the ion intensity over 15 s. The blank intensity was then subtracted from the analyte intensity ($I_A - I_B$). The concentrations of the bracketing standards were adjusted to match those of the sample solutions within 10% (one standard on each side in terms of analyte concentration for intensity interpolation). Two bracketing schemes were investigated (time interpolation and intensity interpolation, Table 2). When no drift with time was observed, the two interpolation schemes gave identical results. When some drift was present, the intensity interpolation gave slightly more precise and accurate results than the time interpolation. For some measurements, intensity interpolation was therefore preferred to time interpolation. The isotopic composition is expressed in δ notation,

$$\delta_j^i = [(^i\text{Fe}/^j\text{Fe})/(^i\text{Fe}/^j\text{Fe})_{STD} - 1] \times 10^3 \quad (1)$$

where ⁱFe and ^jFe are two isotopes of iron and STD refers to the interpolated standard ratio (Table 2). The Fe isotopic standard IRMM-014 was used for normalization. The bracketing was repeated n times ($n \geq 6$). In the intensity interpolation scheme, n should be an even number to avoid any bias. When comparing different studies, it is often more convenient to calculate the fractionation per atomic mass unit. Its value (\hat{F}_j^i) and its uncertainty (given as 95% confidence interval) are calculated as follows,

$$\hat{F}_j^i = \frac{\bar{\delta}_j^i}{i - j} \pm \frac{2s(\delta_j^i)}{(i - j)\sqrt{n}} \left(1 + \frac{20}{n^2}\right) \quad (2)$$

where $\bar{\delta}_j^i$ is the average of the n measurements, i and j represent the masses of the two isotopes, $s(\delta_j^i)$ is the sample standard deviation of the n analyses, and the term $(1 + 20/n^2)$ is a numerical adjustment for small sample sizes.⁴⁷ Note that with bracketing, every standard except for the first and the last, is shared by two samples. This requires that a small correction be applied to the calculated uncertainty. This bias was estimated using Monte Carlo simulations to be <3%. Because ⁵⁷Fe has a persistent contribution from ⁴⁰Ar¹⁶O¹H and ⁵⁸Fe is a very low abundance isotope, the most reliable isotopic ratio is ⁵⁶Fe/⁵⁴Fe.

Two practices coexist in the literature for normalizing the Fe isotopic composition. Most people use the IRMM-014 isotopic stan-

dard¹ distributed by the Institute for Reference Materials and Measurements while some^{8,16} use the average of multiple isotopic analyzes of terrestrial and lunar igneous rocks. The isotopic composition of an IRMM-014 solution prepared by Olivier Rouxel (Woods Hole Oceanographic Institution) was analyzed against the IRMM-014 solution prepared at the Field Museum. As illustrated in Table 3, IRMM-014 is isotopically homogeneous at the level of precision (0.024‰/amu). The Fe isotopic composition of the Orgueil CI1 carbonaceous chondrite, which is the meteorite that best approximates the solar system composition, is indistinguishable from that of IRMM-014 within uncertainties (0.015 ± 0.032 ‰/amu). This result agrees with independent measurements of the same meteorite by Kehm et al.⁸ (0.020 ± 0.078 ‰/amu after conversion from Kil919 to IRMM-014 normalization using ref 16) and Poitrasson et al.¹⁴ (-0.016 ± 0.021 ‰/amu). Taking the weighted ($1/\sigma^2$) average of all these measurements, the Fe isotopic composition of Orgueil is -0.005 ± 0.017 ‰/amu, again indistinguishable from that of IRMM-014. Note that Zhu et al.⁶ had found a different value for Orgueil (0.197 ± 0.017 ‰/amu), and it is unclear at present whether this results from sample heterogeneity. Beard et al.¹⁶ recommended that Fe isotopic compositions be reported relative to lunar and terrestrial igneous rocks, arguing that this is similar to the use of standard mean ocean water for the oxygen isotope system. However, the Fe isotopic compositions of terrestrial mantle rocks may prove to be heterogeneous as analytical capabilities improve²⁴ and lunar igneous rocks have distinct isotopic compositions compared to terrestrial igneous rocks.¹⁴ While for oxygen there is a unique reference standard (Vienna-SMOW), there is no agreement on which mantle material to use for normalization. Because (i) the Fe isotopic composition of IRMM-014 is closer to the cosmic composition than the terrestrial mantle and (ii) IRMM-014 is isotopically more homogeneous than lunar and terrestrial igneous rocks, we propose that Fe isotopic measurements be reported relative to IRMM-014.

Mass-Independent Effects. Except for a few notable exceptions, departure from mass fractionation is typically of limited magnitude. External normalization is not precise enough to detect these small variations. The common procedure is to calculate the extent of mass fractionation based on a pair of reference isotopes and to propagate this correction to other isotopes. Because the pair of reference isotopes can be affected by mass-independent effects, the observed variations must be compared against synthetic spectra.^{48–50} A single law is used to correct for natural and instrumental mass fractionation. Thus, this procedure works only if the laws describing I and N are identical or when I is much larger than N. The most versatile parametric law for describing instrumental and natural mass fractionation is the generalized power law (GPL).^{40,51–53} The exponential law is a special case of the GPL that relates the measured ratio (r) to the true value (R) and the relative mass difference ($\Delta M/M$) as follows,

$$r = R(1 + \Delta M/M)^\beta \quad (3)$$

where the fractionation factor β is a free parameter. Although it

(48) Dauphas, N.; Marty, B.; Reisberg, L. *Astrophys. J.* **2002**, *565*, 640–644.

(49) Dauphas, N.; Marty, B.; Reisberg, L. *Astrophys. J.* **2002**, *569*, L139–L142.

(50) Dauphas, N.; Davis, A. M.; Marty, B.; Reisberg, L. *Earth Planet. Sci. Lett.*, in press.

(47) Berry, D. A. *Statistics, A Bayesian Perspective*; Duxbury Press: Belmont, 1996.

Table 3. Mass-Dependent Iron Isotopic Composition of Reference Materials^a

sample	description	δ_{54}^{56}	δ_{54}^{57}	F (‰/amu)	F reference
IRMM-014	Isotopic standard (WHOI)	-0.030 ± 0.065	-0.066 ± 0.111	-0.018 ± 0.024	0
IF-G	3.8 Ga old BIF (Isua, Greenland)	0.666 ± 0.038	0.976 ± 0.209	0.332 ± 0.018	0.320 ± 0.021^b
DTS-2	Dunite (Twin Sisters, WA)	0.022 ± 0.041	-0.058 ± 0.072	-0.002 ± 0.016	$0.028 \pm 0.035,^b 0.049 \pm 0.014^{14}$
BCR-2	Basalt (Columbia River, WA)	0.054 ± 0.077	0.159 ± 0.212	0.033 ± 0.034	$0.034 \pm 0.018,^{14} 0.044 \pm 0.039^{16}$
AGV-2	Andesite (Lake County, OR)	0.112 ± 0.081	0.165 ± 0.275	0.056 ± 0.037	$0.045 \pm 0.021,^{14} 0.057 \pm 0.036^{16}$
Orgueil	CI1 carbonaceous chondrite (13.69 mg)	0.015 ± 0.074	0.108 ± 0.192	0.015 ± 0.032	$0.020 \pm 0.078,^8 -0.016 \pm 0.021^{14}$

^a IRMM-014 (WHOI) is a solution prepared by Olivier Rouxel from a different batch of the pure metal than that used for normalization (IRMM-014 Field Museum). ^b Olivier Rouxel, personal communication. Note that the reference values for F were obtained on DTS-1, BCR-1, and AGV-1. DTS-2, BCR-2, and AGV-2 were sampled at the same localities. All values are normalized to IRMM-014. When normalized to terrestrial and lunar igneous rocks in the initial publications,^{8,16} the Fe isotopic compositions were converted to IRMM-014 normalization using ref 16. The uncertainties were propagated accordingly. Error bars are 2σ .

does not describe perfectly the mass fractionation in ICPMS,^{40,52} it is close enough to be used in most applications. The fractionation factor is calculated by setting the reference ratio $^{57}\text{Fe}/^{54}\text{Fe}$ to a constant value of 0.362 55.¹ This β factor is then used to calculate the normalized (unfractionated) ratio R^* ($^{57}\text{Fe}/^{54}\text{Fe}$) based on the observed ratio r . The expected variations are small, so the ϵ unit is used to express departure from mass fractionation,

$$\epsilon_j^i = [(^{57}\text{Fe}/^{54}\text{Fe})^*/(^{57}\text{Fe}/^{54}\text{Fe})_{\text{STD}}^* - 1] \times 10^4 \quad (4)$$

where the asterisk indicates that the ratios have been corrected for mass fractionation by internal normalization. Because the fractionation law does not adequately reproduce the instrumental mass fractionation, it is important to combine internal normalization with external standard bracketing as described in the previous section (Table 2 with R^* in place of R). When little drift was present, time interpolation was used. Otherwise, intensity interpolation was preferred. An equation similar to eq 2 can be applied to mass-independent effects,

$$\epsilon_j^i = \epsilon_j^i \pm \frac{2s(\epsilon_j^i)}{\sqrt{n}} \left(1 + \frac{20}{n^2} \right) \quad (5)$$

As in the case of mass fractionation, the denominator isotope is ^{54}Fe ($j = 54$). For mass-independent investigations, the number of repeated measurements was typically greater than 20.

Due to the huge abundance contrast between ^{56}Fe and ^{58}Fe ($^{56}\text{Fe}/^{58}\text{Fe} = 325.48$), measuring all the isotopes of Fe simultaneously is technically challenging. In most configurations, when the ^{58}Fe ion intensity is high enough to be measured at high precision, ^{56}Fe saturates its collector. For this reason, most high-precision investigations of Fe isotope abundances have focused on the three most abundant isotopes, 54, 56, and 57. The few measurements of ^{58}Fe obtained so far have large uncertainties (typically 5ϵ at 2σ).^{8,32,54,55} In the present study, the $10^{11} \Omega$ resistor on the axial collector (^{56}Fe) was replaced by a $10^{10} \Omega$ resistor, to

accommodate ion currents up to 1 nA. Doing so, ^{58}Fe could be measured with high precision (0.5ϵ at 2σ). For measurements of mass-independent effects, the instrument was operated under slightly different conditions from those described previously. Most importantly, the concentration of the analyzed solution was set at 100 ppm. With such concentrated solutions, the cones would clog very rapidly in soft extraction. The measurements were therefore performed in hard extraction, with the slit and extraction lenses adjusted to get 5 V on the axial collector (0.5 nA for ^{56}Fe). The main motivation and benefit of doing that is to increase dramatically the signal-to-noise ratio for all isotopes. The data acquisition protocol is identical to that used in the previous section.

RESULTS

Mass-Dependent Effects. Mass fractionation determinations can potentially be affected by isobaric interferences, matrix elements that could modify the instrumental mass bias, and isotopic fractionation during chemistry. These problems can be addressed by analyzing the Fe isotopic composition after successive passages through the column. Indeed, if the analysis is corrupted by isobaric interferences, it is very unlikely that the contribution of these interferences on the measured isotopes would remain constant after one additional passage. Similarly, if the presence of matrix elements affects instrumental mass bias, the measured isotopic composition should drift toward the true composition as the solution gets cleaner. If column chromatography fractionates Fe isotopes, then the measured isotopic compositions should differ before and after column chemistry.

The samples used for testing the analytical protocol are residues left from vacuum evaporation of molten wüstite and solar compositions. The advantages of analyzing these samples are that they are heavily fractionated and that the measured isotopic compositions can be compared against theoretical expectations. Application of the Hertz–Knudsen equation governing the evaporation of a liquid⁵⁶ leads to the following fractionation factor between the residue and the gas for the isotopes i and j , $\alpha = (\gamma_j/\gamma_i)(m_i/m_j)^{1/2}$, where m_i and m_j are the masses and γ_i and γ_j are the evaporation coefficients. Experiments were performed in a vacuum furnace at the Department of the Geophysical Sciences (The University of Chicago) following protocols described elsewhere.^{57,58} Powder samples of wüstite (FeO) and mixtures of

(51) Dauphas, N. *Icarus* **2003**, *165*, 326–339.

(52) Wombacher, F.; Rehkämper, M. *J. Anal. At. Spectrom.* **2003**, *18*, 1371–1374.

(53) Albarède, F.; Telouk, P.; Blichert-Toft, J.; Boyet, M.; Agranier, A.; Belson, B. *Geochim. Cosmochim. Acta* **2004**, *68*, 2725–2744.

(54) Rotaru, M.; Birck, J.-L.; Allègre, C. J. *Nature* **1992**, *358*, 465–470.

(55) Podosek, F. A.; Nichols, R. H.; Brannon, J. C.; Ott, U. *Lunar Planet. Sci.* **1997**, *XXVIII*, 121.

(56) Davis, A. M.; Richter, F. M. In *Meteorites, Comets, and Planets. Treatise on Geochemistry I*; Elsevier-Pergamon: Oxford, 2003; pp 407–430.

(57) Hashimoto, A. *Nature* **1990**, *347*, 53–55.

Table 4. Mass-Dependent Iron Isotopic Composition of Vacuum Evaporation Residues^a

	WU					
	1	2	3	4	5	6
<i>f</i>	0.974	0.684	0.410	0.540	1.000	0.258
<i>F</i> (0)		3.97	8.70		0.06	12.59
<i>F</i> (1)	0.28	3.97	8.72	6.19	0.06	12.56

	SCR							
	7	8	9	10	12	18	20	22
<i>f</i>						0.040	0.008	0.536
<i>F</i> (1)	3.79	12.11	0.52	18.46	16.18			0.251
<i>F</i> (2)	3.67	12.10	0.48	18.54	16.09	21.46	32.15	10.61

^a WU and SCR refer to wüstite and solar starting compositions. The WU 1–6, SCR 7–12, and SCR 18–22 series were evaporated at 1823, 1823, and 1973 K, respectively. *f* is the fraction of ⁵⁴Fe remaining after evaporation. The isotopic composition *F* is given in ‰/amu and was calculated based on the ⁵⁶Fe/⁵⁴Fe ratio (eqs 1 and 2). The number of passages through the column are indicated in parentheses for each composition. The precision (95% confidence limit) is typically <0.1‰/amu. The uncertainty on *f* is 0.1 for the WU series and 15% relative for the SCR series.

oxides in close to solar proportions (24.3 wt % MgO, 2.8% Al₂O₃, 34.1% SiO₂, 1.9% CaO, and 36.8% FeO) were suspended in an Ir wire in a resistance-heated chamber. The pressure in the vacuum furnace was $(1-5) \times 10^{-9}$ atm. The run temperatures were set at 1823 K (WU 1–6 and SCR 7–12) and 1923 K (SCR 18–22). The duration of the experiments ranged from 0 to 25 200 s. For wüstite evaporation experiments, the fraction of Fe lost was determined by measuring the mass loss. Interpretation of solar evaporation experiments run at 1823 K (SCR 7–12) is not straightforward due to chemical and textural heterogeneity of the run products (poikilitic olivine crystallized and segregated during the run). For the solar evaporation experiments run at 1923 K (SCR 18–22), the fraction of Fe lost was determined by calculating the Fe/(Al + Ca) ratio of the starting material and the residues from 2000 to 3000 SEM-EDS spot analyses of each sample. The results are reported in Table 4.

Because wüstite contains only Fe and O, its composition can be measured without chemistry and after one passage through the column. For some solar evaporation experiments, the isotopic composition was measured after one as well as after two passages through the column. The isotopic compositions before and after column chromatography for the WU and SC series are identical. This is illustrated in Figure 2, where the intercept of the correlation line is -0.047 ± 0.055 ‰/amu (indistinguishable from 0) and its slope is 1.003 ± 0.006 (indistinguishable from unity). The external reproducibility, including column chemistry and analysis, is estimated to be better than 0.1‰/amu. The results can also be compared against theory in the case of wüstite. If the isotopic composition of the residue follows a Rayleigh distillation then,

$$\ln(R/R_0) = (1 - 1/\alpha)(-\ln f) \quad (6)$$

where *f* is the fraction remaining of the denominator isotope (⁵⁴Fe) and α is the fractionation factor between the residue and the gas. It has been shown that, during prolonged evaporation of FeO, the isotopic composition of the residue follows a Rayleigh dis-

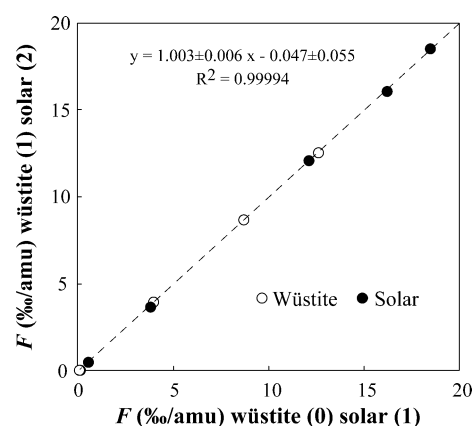


Figure 2. Iron isotopic composition of evaporation residues after *n* and *n* + 1 passage(s) through anion-exchange columns (the number of passages are indicated in parentheses in the axes labels). The slope is equal to unity (1.003 ± 0.006) and the intercept is equal to zero (-0.047 ± 0.055 ‰/amu) within uncertainties. The Fe isotopic compositions before and after column chromatography are therefore identical.

tillation with a fractionation factor that scales to the square root of the masses⁵ ($\gamma_j = \gamma_i$). The expected fractionation factor for the ⁵⁶Fe/⁵⁴Fe ratio is $(56/54)^{1/2} = 1.01835$. That measured by SIMS is 1.0183.⁵ The value we derive here (Figure 3a) is 1.01877 ± 0.00047 , in complete agreement with theory and earlier measurements. For the solar evaporation experiments at 1923 K (Figure 3b), the Fe isotopic composition also follows a Rayleigh distillation but with a fractionation factor for the ⁵⁶Fe/⁵⁴Fe ratio, 1.01322 ± 0.00067 , that is lower than the theoretical prediction. This is reminiscent of what has been observed for magnesium⁵⁹ and emphasizes the importance of determining experimentally the fractionation factors when investigating evaporative processes.

Various reference materials have been analyzed (IF-G, DTS-2, BCR-2, AGV-2) and the data agree with results obtained in other laboratories for the same rocks (Table 3).

Mass-Independent Effects. With measurements of mass-independent effects, it is crucial to eliminate direct isobaric interferences. For this reason, the anion-exchange chromato-

(58) Wang, J.; Davis, A. M.; Clayton, R. N.; Hashimoto, A. *Geochim. Cosmochim. Acta* **1999**, *63*, 953–966.

(59) Janney, P. E.; Mendybaev, R. A.; Dauphas, N.; Davis, A. M.; Richter, F. M.; Wadhwa, M. *Lunar Planet. Sci.* **2004**, XXXV, 2092.

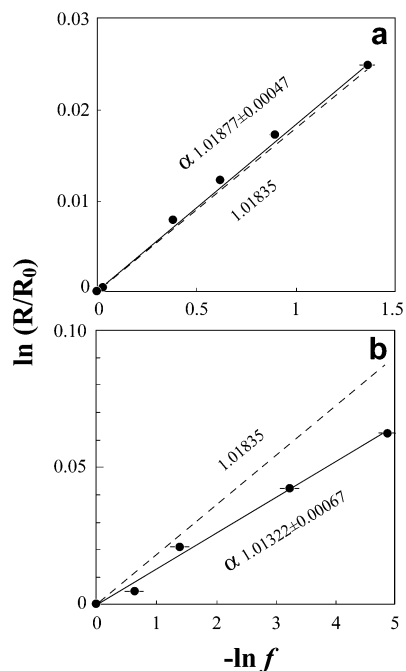


Figure 3. Determination of the fractionation factor α for vacuum evaporation of wüstite composition at 1823 K (a) and solar composition at 1973 K (b). R is the $^{56}\text{Fe}/^{54}\text{Fe}$ ratio ($(^{56}/^{54})^{1/2} = 1.01835$). In this diagram, Rayleigh distillation is represented as a straight line with a slope equal to $1 - 1/\alpha$ (eq 6).

graphic separation was repeated 3 times, with matrix elution volumes of 15, 25, and 25 mL of 6 M HCl, respectively. Various terrestrial and extraterrestrial rocks were analyzed to validate the method and search for natural mass-independent effects. Note that no mass-independent effects are expected for terrestrial igneous samples and they may thus be used to test the accuracy of the protocol. Along with metallic iron inclusions in basalts from Disko (Greenland), josephinite (Ni_2Fe to Ni_3Fe) from Josephine Creek (JO, USA) is one of the few occurrences of natural metallic iron or nickel–iron alloy on Earth. The main motivation for analyzing Josephinite was to test whether Fe isotopes could be precisely measured in Ni-rich samples. Indeed, ^{58}Ni , which is the most abundant isotope of Ni (68.0769%), can potentially interfere with ^{58}Fe , the least abundant isotope of Fe (0.282%). If Ni had not been separated from Fe in this sample, this would have resulted in a $6 \times 10^4\epsilon$ direct interference at mass 58. As illustrated in Figure 4, the Fe isotopic composition of this sample is within 0.3ϵ and 0.5ϵ of the terrestrial composition for the $^{56}\text{Fe}/^{54}\text{Fe}$ and $^{58}\text{Fe}/^{54}\text{Fe}$ ratios, respectively. An anhydrous lherzolite collected by Reika Yokochi in Eifel, Germany (DD5) was analyzed to test the separation of Fe from a silicate matrix. Again, the measured composition is identical within uncertainties to that of the standard solution. This demonstrates the accuracy of the method, which is 1 order of magnitude more precise than what had been achieved before^{8,32,54,55} (0.5ϵ vs 5ϵ for ^{58}Fe).

Archaean rocks show mass-independent isotope effects for S.³¹ The interpretation is that, with no ozone shield at that time, the atmosphere was transparent to deep UV radiation that could photodissociate SO_2 – SO , a mechanism that is known to create mass-independent isotopic effects. Photooxidation of hydrated ferrous iron in oceans overlain by a transparent atmosphere might have caused the precipitation of banded iron formations in the

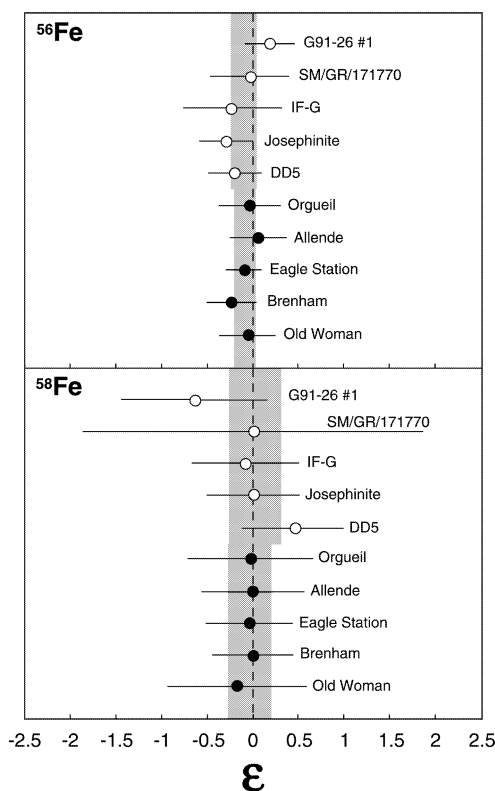


Figure 4. Mass-independent variation of the Fe isotopic composition ($^{56}\text{Fe}/^{54}\text{Fe}$ and $^{58}\text{Fe}/^{54}\text{Fe}$ ratios) after internal normalization ($^{57}\text{Fe}/^{54}\text{Fe} = 0.36255$).¹ Empty circles, terrestrial samples. Filled circle, extraterrestrial samples. The gray areas are the uncertainty intervals of the weighted averages. See Table 5. Uncertainties are 2σ .

Archaean.⁶⁰ It is possible that such a mechanism could induce mass-independent effects. IF-G is a geostandard prepared from a large iron ore deposit in the 3.8-Ga-old Isua supracrustal belt, west Greenland.^{61,62} G91–26 No. 1, also known as ANU92–197, is a banded quartz–pyroxene rock of disputed origin^{63–67} collected by Allen Nutman at Akilia (Greenland). SM/GR 171770 is a quartz–pyroxene rock collected by Stephen Moorbath at Innersuartuut (island 10 km south of Akilia, Greenland). No exotic effects have been observed in these rocks.

Except for the notable exception of oxygen, the isotopic compositions of major elements in meteorites are remarkably homogeneous. Searches for mass-independent effects for Fe in bulk meteorites have been limited to the most abundant isotopes 54, 56, and 57,⁶ or have been plagued by large uncertainties on 58.^{8,32,54,55} The CV3.2 Allende chondrite and the Eagle Station Pallasite are thought to have formed in the same region of the protosolar disk that was characterized by extremely anomalous

(60) Braterman, P. S.; Cairns-Smith, A. G.; Sloper, R. W. *Nature* **1983**, *303*, 163–164.

(61) Govindaraju, K. *Geostand. Newsl.* **1980**, *8*, 63–112.

(62) Govindaraju, K. *Geostand. Newsl.* **1995**, *19*, 55–95.

(63) Mojzsis, S. J.; Arrhenius, G.; McKeegan, K. D.; Harrison, T. M.; Nutman, A. P.; Friend, C. R. L. *Nature* **1996**, *384*, 55–59.

(64) Fedo, C. M.; Whitehouse, M. J. *Science* **2002**, *296*, 1448–1452.

(65) Mojzsis, S. J.; Harrison, T. M. *Science* **2002**, *298*, 917a (Technical Comments).

(66) Friend, C. R. L.; Nutman, A. P.; Bennett, V. C. *Science* **2002**, *298*, 917a (Technical Comments).

(67) Fedo, C. M.; Whitehouse, M. J. *Science* **2002**, *298*, 917a (Technical Comments).

isotopic compositions compared to average solar system material.⁴⁸ They therefore appear to be the most promising candidates to search for isotope anomalies in bulk meteorites. As illustrated in Figure 4, the Fe isotopic compositions of these two meteorites are normal within uncertainties (0.2ϵ for 56 and 0.5ϵ for 58). Kehm et al.⁸ reported a marginal departure from mass fractionation for the main group pallasite Brenham and IIAB iron meteorite Old Woman. Analyses presented here demonstrate that these two objects have normal Fe isotopic compositions (Figure 4). The bulk Fe isotope composition of the CI1 Orgueil carbonaceous chondrite, representative of the average solar system composition, is also normal. These results suggest that the Fe isotopic composition of the solar nebula was uniform at the scale of small planetesimals.

CONCLUSIONS

New chemical and mass spectrometric procedures have been developed for analyzing the mass-dependent and -independent isotopic compositions of Fe in natural samples. It is shown that the chromatographic separation of Fe from matrix and isobar elements described here does not fractionate its isotopic composition within $0.02\text{‰}/\text{amu}$ at 2σ . Tests performed on heavily fractionated evaporation residues validate the protocol. The isotopic composition of Fe left after prolonged evaporation of wüstite composition follows a Rayleigh distillation with a fractionation factor that is equal to the square root of the masses of the isotopes. This is in agreement with earlier results and theoretical expectation. In the case of evaporation of Fe from a complex mixture of oxides, the residue also follows a Rayleigh distillation but with a fractionation factor that is lower than that expected (1.01322 ± 0.00067 versus 1.01835 for the 56–54 pair). Various geostandards have been analyzed, and the measured Fe isotopic compositions all agree with results obtained in other laboratories on the same samples. More importantly, within analytical uncertainty for measurements in three laboratories, the iron isotopic composition of the IRMM-014 reference material is identical to the best available sample of bulk solar system composition, the Orgueil meteorite.

A similar procedure is used for analyzing the mass-independent isotopic composition of Fe. The isotopic compositions of some terrestrial rocks, including josephinite (Josephine Creek, USA) and an anhydrous lherzolite (Eifel, Germany), are shown to be normal within uncertainties. This demonstrates that the mass-independent isotopic composition of Fe can be measured accurately with precisions of 0.2ϵ and 0.5ϵ at 2σ for ^{56}Fe and ^{58}Fe , respectively. The precision obtained for ^{58}Fe is 1 order of magnitude better than what had been achieved before. This procedure is applied to samples that could potentially exhibit mass-independent effects (terrestrial Archaean rocks and meteorites). Banded iron formations and quartz-pyroxene rocks from Isua,

Table 5. Mass-Independent Iron Isotopic Compositions of Terrestrial and Extraterrestrial Samples^a

	$\epsilon^{57}\text{Fe}$	$\epsilon^{58}\text{Fe}$
G91–26 No.1	0.18 ± 0.27	-0.64 ± 0.79
SM/GR/171770	-0.03 ± 0.43	0.00 ± 1.86
IF-G	-0.23 ± 0.53	-0.09 ± 0.59
Josephinite	-0.29 ± 0.28	0.00 ± 0.50
DD5	-0.20 ± 0.29	0.45 ± 0.55
Orgueil	-0.03 ± 0.33	-0.03 ± 0.68
Allende	0.05 ± 0.30	-0.01 ± 0.55
Eagle Station	-0.09 ± 0.19	-0.05 ± 0.47
Brenham	-0.23 ± 0.26	-0.01 ± 0.44
Old Woman	-0.05 ± 0.30	-0.18 ± 0.75

^a G91–26 No. 1, also known as ANU92–197, is a banded quartz-pyroxene rock of disputed origin^{63–67} collected by Allen Nutman at Akilia (Greenland). SM/GR 171770 is a magnetite-rich quartz-pyroxene rock collected by Stephen Moorbath at Innersuartuut (island 10 km south of Akilia, Greenland). IF-G is a 3.8-Ga-old banded iron formation from Isua (Greenland). Josephinite is a natural terrestrial iron–nickel alloy from Josephine Creek. DD5 is an anhydrous lherzolite collected by Reika Yokochi in Eifel, Germany. Orgueil and Allende are CI1 and CV3.2 carbonaceous chondrites, respectively. Eagle Station and Brenham are Eagle Station and main group pallasites, respectively. Old Woman is a IIAB iron meteorite. Uncertainties are 2σ .

Akilia, and Innersuartuut (Greenland) do not show any departure from mass-dependent fractionation. Similarly, the Allende CV3.2 and Orgueil CI1 chondrites, the Eagle Station and Brenham pallasites, and the Old Woman IIAB iron meteorite are normal within uncertainties. This suggests that Fe isotopes were thoroughly homogenized in the solar system on the scale of planets and planetesimals.

ACKNOWLEDGMENT

This work benefited from many fruitful discussions with O. Rouxel, R.N. Clayton, R.S. Lewis, and R. Yokochi. We thank Stephen Moorbath and Reika Yokochi for providing us the G91-26 No. 1 (SM), SM/GR/171770 (SM), and DD5 (RY) samples. This work was supported by the National Aeronautics and Space Administration and National Science Foundation through Grants NAG5-12997 (to A.M.D.), NAG5-13027 (to F.M.R.), NAG5-12077, NAG5-7196, and EAR-9871154 (to M.W.). We thank two anonymous reviewers for thorough and constructive reviews.

Note Added after ASAP. The paper was posted on the Web on 8/27/04. An error in the Table 2 equations was noted and corrected. The paper was reposted on 9/15/04.

Received for review February 21, 2004. Accepted June 23, 2004.

AC0497095